Iraqi Journal of Physics, 2024
https://doi.org/10.30723/ijp.v22i3.1229

Vol. 22, No. 3, PP. 37-49
P-ISSN: 2070-4003
E-ISSN: 2664-5548

Synthesis and Characterization of Gold Nanoparticles and Gold Nanoparticles Loaded with Bromelain

Haneen Ibrahim Ali[1a*] and Baydaa H. Mutlak[1b]
[1]*Department of Biology, College of Education for Pure Science (Ibn Al-Haitham), University of Baghdad, Baghdad, Iraq*
[b]E-mail:baydaahussein@gmail.com
[a*]Corresponding author: haneen.i.ali@aliraqia.edu.iq

Abstract

The production and use of nanometallic elements, such as gold, have received a lot of attention lately due to their distinctive features and wide range of uses. Most of these studies have employed the Turkevich approach. This research employed the Turkevich technique to produce gold nanoparticles (AuNPs). AuNPs and bromelain-loaded AuNPs were characterized using a variety of methods, including ultraviolet-visible spectroscopy (UV-Vis), Fourier transform infrared spectroscopy (FTIR), field emission scanning electron microscopy (FE-SEM), X-ray diffraction (XRD), transmission electron microscopy (TEM), and zeta potential (ZP) measurements. The UV-Vis spectra of bromelain, AuNPs, and AuNPs-bromelain each had a peak at 276, 534, and 550 nm wavelengths, respectively. The FE-SEM and TEM studies revealed the presence of spherical particles with a smooth surface. The diameters of the AuNPs ranged from 49.32 to 77.29 nm; the diameters of the bromelain-AuNPs ranged from 46.39 to 75.66 nm, as determined by the FE-SEM analysis. The TEM analysis indicated that the particles' sizes ranged from 7.40 to 15 nm for AuNPs and 14.51 nm for AuNPs-bromelain. The XRD patterns revealed numerous diffraction peaks, indicating the crystal structure of the synthesized nanoparticles. FTIR spectrometry was employed to identify the functional groups in the synthesized nanoparticles. Zeta potential (ZP) measurements revealed that AuNPs had a zeta potential value of +0.1±0.4, and the zeta potential value for AuNPs-bromelain was +1.2±3.0 mV.

Article Info.

Keywords:
Bromelain, AuNPs, X-Ray Diffraction, Zeta Potential, Transmission Electron Microscopy

Article history:
Received: Jan. 01, 2024
Revised: May, 17, 2024
Accepted: May, 21,2024
Published: Sep. 01,2024

1. Introduction

1.1. Nanotechnology

Nanotechnology, which broadly refers to the design, fabrication, and manipulation of particle structures from 1-100 nm, has quickly gained ground in contemporary study [1-3]. The technology has advanced significantly since its beginnings. It has gained significance in a variety of field domains like health care, food, cosmetics, pharmaceuticals delivery, chemical industries, electronics, space industries, energy science, optoelectronic devices, single-electron transistors, and photo uses for electrochemistry [4, 5]. One of the first metals to be uncovered was gold [6]. Early reports on colloidal gold may have been written by Indian, Chinese, and Arabic scientists working to produce the substance as early as the fifth and fourth centuries [7]. Scientists used colloidal gold for therapeutic and other purposes. Colloidal gold was studied and used in all European chemistry research facilities [8]. Various chemicals, such as citric acid, alkanethiols, amines, surfactants and organic polymers, have been used to stabilize reactive gold nanoparticles in solutions. Using alkanethiols, in particular, constituted an important breakthrough in the development of small (1-3nm) gold nanoparticles [9].

Gold nanoparticles (AuNPs) are prepared by various synthetic techniques, including chemical reduction, photolysis or radiolysis, ultrasonic reduction, etc [10, 11]. The most common chemical method for creating AuNPs is the well-known Turkevich method, which is one of the most promising approaches compared to others. In this method, citrate [12], ascorbic acid [13], or tannic acid [14] are used as mild reducing agents to reduce the Au^{+3} ions. The Turkevich approach is used to create biocompatible and compact AuNPs; it is vital to regulate several parameters such as pH, temperature, and concentration [15]. Brust and Schiffrin introduced the Brust-Schiffrin technique in 1944. The regulated and low dispersion thermally stable and air-stable AuNPs can be easily synthesized using this technology. This procedure involved transferring $AuCl_4$ from an aqueous phase to toluene utilizing tetraoctylammonium bromide (TOAB) as a phase-transfer agent and reducing it with $NaBH_4$ in the presence of dodecanethiol. The organic phase changes color from orange to deep brown when the reducing chemicals are used [16].

Nanoparticles have been used for drug delivery, especially in the treatment of the medical field, but the controversy continues about their cytotoxicity. Numerous studies have shown the AuNPs adaptability as an essential drug delivery system. Drug delivery has become a very effective way to convey medication without compromising its safety or effectiveness. Drugs are typically administered by cutaneous, nasal, oral, ocular, rectal, buccal, and inhalation, among other popular delivery methods. Several biomolecules, including proteins, antibodies, peptides, genes, and vaccines, could potentially be degraded by the organisms when supplied using the aforementioned techniques. Numerous alternative drug delivery techniques were created to improve the reproducibility, reliability, sensitivity, and specificity in the intended locations. Rapidly dissolving hydrophilic polymers were used in thin film drug delivery, and they were quickly absorbed when they came in touch with the buccal cavity. Histopathological studies revealed the non-toxic and protective effect of the AuNPs on the vital organs, and they can be used to ameliorate hyperglycemia and oxidative stress. The study contrasted the ability of AuNPs to produce acute systemic toxicity in response to oral insults [17-19].

1.2. A Description of Bromelain

Pineapple (Ananas comosus) is an edible member of the family Bromeliaceae and is grown in several tropical and subtropical countries, including Mexico, Philippines, Thailand, Indonesia, Malaysia, Kenya, India and China. It has been used as a medicinal plant in several native cultures. Its medicinal qualities are attributed to bromelain, which is a crude extract from pineapple that contains, among other compounds, various closely related proteinases exhibiting various fibrinolytic, antiedematous, antithrombotic, and anti-inflammatory activities in vitro and in vivo. Bromelain has been chemically known since 1875 and is used as a phytomedical compound [20-23].

2. Experimental Work

2.1. Preparation of Bromelain Solution

Bromelain solution was prepared by dissolving it in deionized water with a final concentration of 10 mg/ml and 30 mg/ml in a beaker conical was placed on a magnetized shaker at room temperature and then filtered and sterilized using paper 0.22μm filtration [24].

2.2. Preparation of Trisodium Citrate Solution

Trisodium citrate solution was prepared by dissolving 0.5 g of trisodium citrate in 50 ml of sterile distilled water.

2.3. Preparation of Gold Solution

This solution was prepared by dissolving 1g of $HAuCI_4.3H_2O$ in 100 mL of double distilled water. The final gold solution of 25 mM concentration (stock solution) was stored in a dark container in a refrigerator [25].

2.4. Synthesis of Gold Nanoparticles

To synthesize gold nanoparticles a 1.4 ml of trisodium citrate solution was mixed with 70 ml of boiling gold solution.

2.5. Synthesis of Gold Nanoparticles Loaded with Bromelain (AuNPs-Bromelain)

Bromelain was loaded onto the gold nanoparticles prepared using the chemical reduction method; this was done by mixing 1 mL of bromelain solution at a concentration of 100 mg/ml with 5 mL of gold nanoparticles solution with stirring on a magnetic vibrating plate for two minutes. The solution was then stored until it was needed [26].

2.6. Characterization of Gold Nanoparticles

2.6.1. Ultraviolet-Visible (UV-Vis) Spectrophotometry

The absorption spectra of gold nanoparticles loaded with bromelain (AuNPs-Bromelain) were measured by an ultraviolet-visible spectrophotometer (type UV-1900i) at room temperature, with ranges from 100 to 1100 nm; distilled deionized water was used as a reference solution [27].

2.6.2. Fourier Transform Infrared (FTIR) Spectroscopy

To identify the effective aggregates of bromelain solution, AuNPs, and AuNPs-BR, an infrared spectrometer (Shimadzu\1800\Jaban), in a wavelength range between 400 - 4000 cm^{-1}. Test pellets were prepared by using one drop of sample and pressed into a disk. These disks were scanned from 4000 to 400 cm-1 to obtain the FT-IR spectra.

2.6.3. Scanning Electron Microscopy (SEM)

A SEM was used to identify the shape and size of particles in the AuNPs and AuNPs-Bromelain solutions separately. Five microliters of solutions were prepared for examination on a gold-plated scanning electron microscope stand and carbon clip. The samples were left at room temperature until dry and examined using different microscope powers [28].

2.6.4. Transmission electron microscopy (TEM)

TEM images were captured using a 400 kV JEOL JEM-1010 (JEOL Ltd., Japan) TEM system. The samples were sonicated for 30 min. A drop of colloidal solution was placed on a copper grid coated with a thin amorphous carbon film on filter paper. The samples were air-dried and held under vacuum in the desiccator before being placed on the specimen holder. Particle size, composition, and distribution of AuNPs and AuNPs-Bromelain were determined [27].

2.6.5. X-Ray Diffraction (XRD)

The crystal structure of AuNPs and AuNPs-bromelain was revealed using an XRD. The sample was prepared by placing nano-gold and bromelain loaded nano-gold particles solutions on glass slides, dried at 100°C and analyzed by XRD. This was done by shining Cu Kα radiation at an angle of 2θ ranging from 20 - 80 degrees and a wavelength (λ = 1.54 Å), at a potential difference of 40 KV and an electric current of 30 mV, the crystal size of AgNPs was calculated [26].

2.6.6. Zeta Potential Measurement

To predict the stability of AuNPs and AuNPs-bromelain prepared according to the chemical method, their zeta potentials were measured using a Zetasizer Nano particle analyser (Zen3600), which operates at a voltage of -150 to wave at 200 mV. The sample

was prepared by mixing gold nanoparticles with distilled water at a ratio of 1:10 in a total volume of one mL, then the sample was loaded into an oil cell for examination at a temperature of 25^{o}C temperature, then the data was recorded as a graph [28].

3. Results and Discussion

3.1. Preparation of Gold Nanoparticles (AuNPs) and Bromelain Loaded Gold Nanoparticles (AuNPs-Bromelain)

The color change is the first sign that gold nanoparticles were created because sodium trisodium citrate reduces the Au+ gold ion into Au atoms. These atoms then act as nucleation sites to speed up the reduction of the remaining gold ions in the $HAuCL_4.3H_2O$ solution; following this, the reduction agent (TCS) triggers the self-assembly of these atoms, forming groups of metal atoms. The resulting solution's color is determined by the size and shape of the formed molecules. The color change of the gold nanoparticle solution from pale yellow to wine red (Fig. 1) may indicate the success of loading bromelain onto the gold nanoparticles. The color change in the solutions could be attributed to a difference in the electronic density of the particles, which could result from a change in the size of the nanoparticles. In the study of Jana et al., the solution underwent a color transition within a few minutes, changing from yellow to black and subsequently to either red or purple, depending on the size of the nanoparticles [29]. Long et al. showed that the gold nanoparticle synthesis process was initiated and completed rapidly within a 22-hour incubation period [30].

Figure 1: The color change in the process of manufacturing gold nanoparticles.

3.2. Characterization of Gold Nanoparticles

3.2.1. (UV–Vis) Spectrophotometry

The UV-visible spectroscopy results were used to confirm the synthesis of the AuNPs and their conjugation with bromelain. Each of the bromelain, AuNPs, and AuNPs-bromelain UV-Vis spectra was characterized of having a peak at wavelengths of 276, 534, and 550 nm, respectively (Fig. 2). These wavelengths confirm the presence of gold and the formation of gold nanoparticles because the absorption peaks at wavelengths in the 500-600 nm range are within the colloidal spectrum of gold nanoparticles [4].

If the absorption peak of the gold nanoparticle solution goes up after the bromelain solution was added, it could mean that the nanoparticles are getting bigger; this is because the size and shape of the nanoparticles affect how intense the absorption is; the absorption peak's value is directly proportional to that [31].

Surface plasmon resonance happens when electrons in the conduction band move back and forth in sync close to the surfaces of nanoparticles. The type of interactions between the gold surface atoms and the surface coating, along with the thickness of the surface coating, influence the position of the surface plasmon resonance peak of the gold nanoparticles [32, 33].

The data reported here is consistent with the particle size distribution analyzed using UV-Vis spectroscopy; setting the pH at an ideal value of 5 produces gold nanoparticles that exhibit high uniformity and a distinct surface plasmon peak at 520 nm [34].

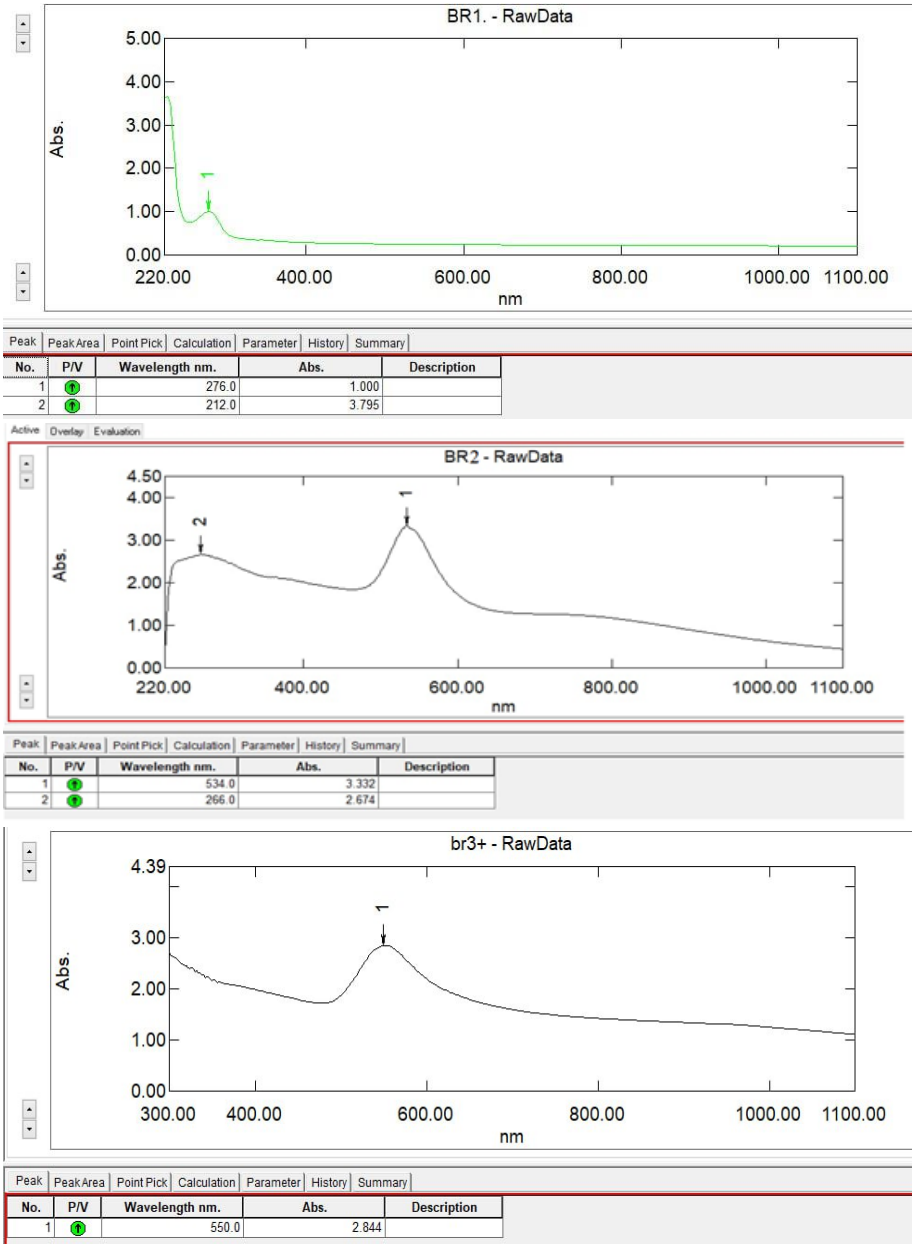

Figure 2: UV-Vis spectra of bromelain, AuNPs and AuNP-bromelain.

3.2.2. FTIR

FTIR is used to determine the intensity of infrared radiation as a function of frequency or wavelength and to distinguish the chemical structures; it could provide information about covalent bonds and identify functional groups. The FTIR analysis is also used to investigate the adsorption of organic species on metal oxide nanoparticles [35, 36]. Fig. 3a illustrates the FTIR spectrum of the bromelain solution; the peaks at frequencies 3410.18 and 3653.18 cm^{-1} indicate the presence of the OH group of alcohol and phenol compounds. Fig. 3b represents the FTIR spectrum of gold nanoparticles loaded with bromelain. The absorption peak at frequency 3305.99 cm^{-1} indicates the presence of the OH group of alcohol and phenol, and the absorption peak at frequency

1535.34 cm^{-1} represents the presence of secondary amine and amide groups. The FTIR spectrum of the synthesized AuNPs, as shown in Fig. 3c, shows a broader peak at 3271.27 cm^{-1} assigned to the O-H stretching of alcohol and phenol compounds. The results presented here agree with earlier previous research [37, 38].

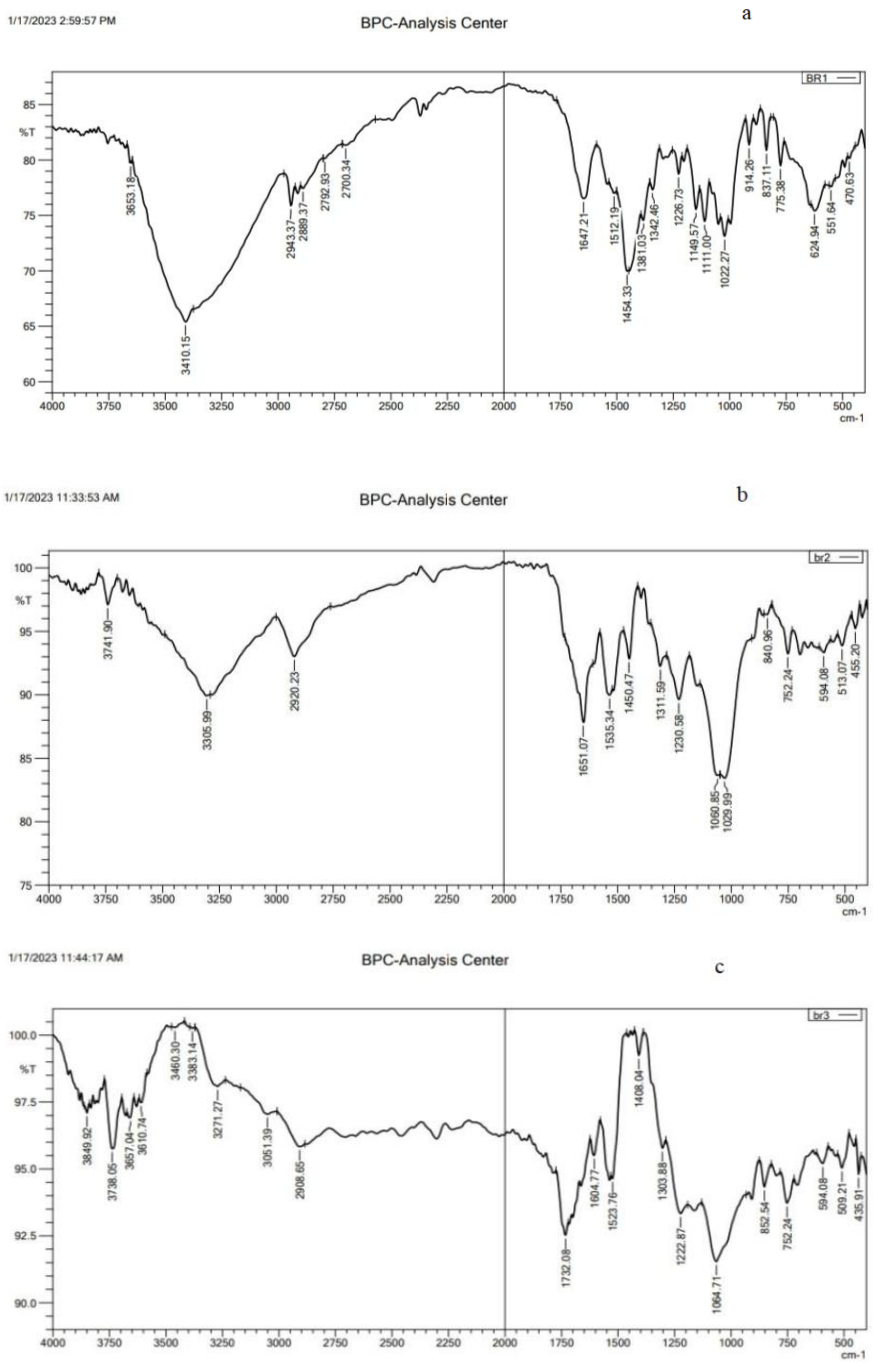

Figure 3: FTIR spectra of (a) Bromelain (b) AuNPs-Bromelain (c) AuNPs.

The spectroscopic analysis of the bromelain solution and the gold nanoparticles loaded with bromelain revealed the presence of O-H groups specific to alcoholic compounds and phenolics, as well as active groups specific to amino compounds in both spectra. This could show that the gold nanoparticles loaded with bromelain contain natural parts of the bromelain solution, which indicates the loading of bromelain onto the gold nanoparticles [39].

This result agrees with that of Parodi et al., whose results on the infrared spectroscopy examination of bromelain and silica nanoparticles loaded with bromelain showed that the spectrum of silica nanoparticles included functional groups specific to bromelain. It is evidence of the success of the bromelain loading process [40].

Sharma and Sharma showed through the results of the infrared spectroscopic examination of the nanoformulation after adding bromelain that the composition contained some peaks that indicate the association of bromelain with the nanoformulation [41]. Abdulghani and Mohuee showed that the formation of a metallic surface was supported by the quality (characteristic vibration bands) of the IR spectrum [42]. Bélteki et al. showed that citrate ions establish weaker interactions with the surface of AuNPs through several carboxylate groups, such as Au-O, in the citrate molecule; these binding are not as strong as the ones produced between AuNPs surfaces and molecules [43].

3.2.3. FE-SEM and TEM

The particle morphology images were obtained using FE-SEM and TEM to further understand the morphological characteristics of AuNPs and AuNPs-bromelain. Fig. 4a depicts the FE-SEM images of particle morphologies of AuNPs, which had an essentially regular, spherical form and sizes ranging from 49.32 to 77.29 nm. The AuNPs emerged as smooth, well-separated structures, which explains the formation of uniformly shaped spherical particles [44-46]. Fig. 4a shows the AuNPs size distribution histogram.

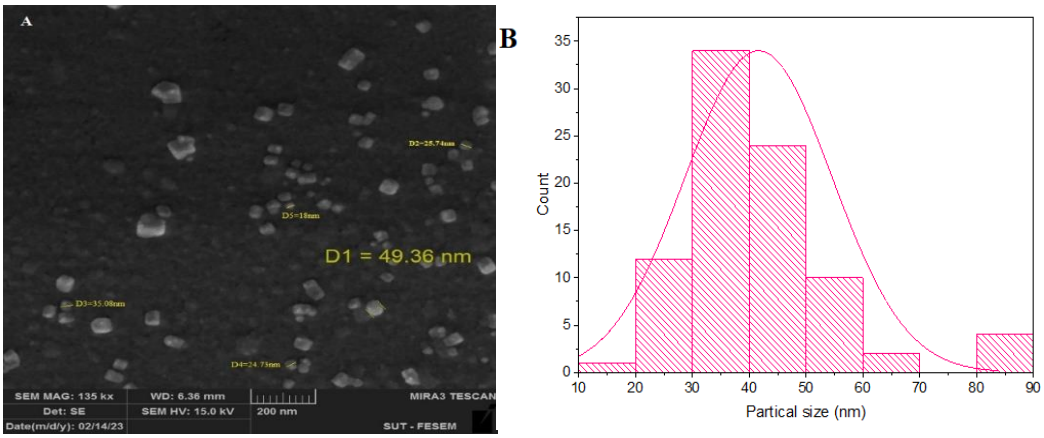

Figure 4: FE-SEM images for (A) AuNPs with scale bar 200nm, (B) particle size distribution histogram.

Fig. 5a depicts SEM images of AuNPs-bromelain showing their morphological properties. The structure of AuNPs-bromelain was noted to have a spherical form and an uneven distribution of particles with sizes ranging from 46.39 to 75.66nm. Fig. 5b shows the AuNPs-bromelain size distribution histogram.

The examination reveals the change in the average size of the nanoparticles before and after loading the bromelain; this confirms the loading of bromelain onto the gold nanoparticles. Note that the bromelain did not alter the shape of the nanoparticles upon loading. This is evident from the preservation of gold minutes. The nanoparticles have a dominant spherical shape, and adding bromelain did not cause agglomeration of the nanoparticles.

Sharma and Sharma study has shown that loading the bromelain enzyme onto various nanoparticles did not change their general appearance [41]. The results of the field emission scanning electron microscope examination showed that the structure of

the nanostructure loaded with bromelain was spherical in shape and had a uniform distribution. In addition, Bhatnagar et al. developed a nanostructure loaded with bromelain. The shapes of the nanoparticles loaded with bromelain were spherical with a uniform distribution, consistent with the current study [46].

The findings of this study are in line with those of Hawar et al., which involved the development of a nano lipid formulation loaded with bromelain to treat rheumatoid arthritis [45].

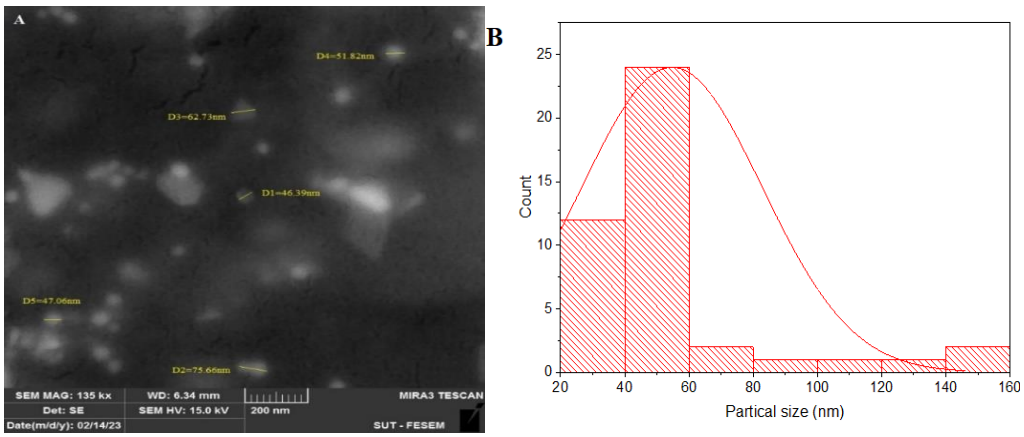

Figure 5: FE-SEM images for (a) AuNPs-bromelain with 200nm scale bar (b) particle size distribution histogram.

Fig. 6a depicts TEM images of the AuNPs. It shows that the AuNPs were well-distributed in form and size, ranging from 7.40 to 15 nm. Most of the AuNPs were seen to be spherical. This is in agreement with the results of Jassim et al. [47]. Fig. 6b shows AuNPs size distribution histogram.

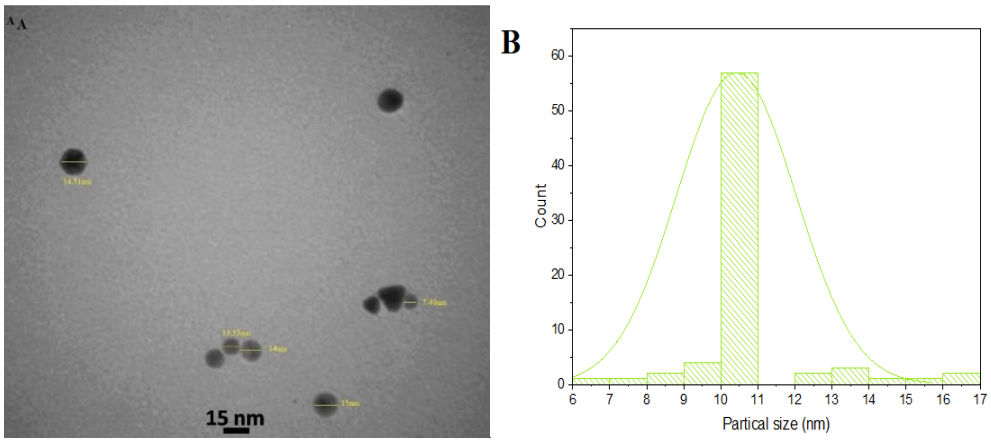

Figure 6: TEM analysis for (a) AuNPs with 15nm scale bar (b) particle size distribution histogram.

A surface morphological study of AuNPs-bromelain in the TEM images showed the formation of spherical particles. The average particle diameter of the colloidal gold was 14.51 nm, with very few particles of higher and lower size distribution. Some AuNPs-bromelain nanostructures appeared with sharp edges and triangular shapes (Fig. 7 a, b, c).

According to Jassim et al., the relatively large size of Br-AuNPs, as observed in TEM images, indicated the attachment of the bromelain to AuNPs surface [48].

Sharma et al. studied the growth mechanism in the citrate reduction of gold (III) salt and proved via TEM the formation of the Au nanoparticle intermediate [49].

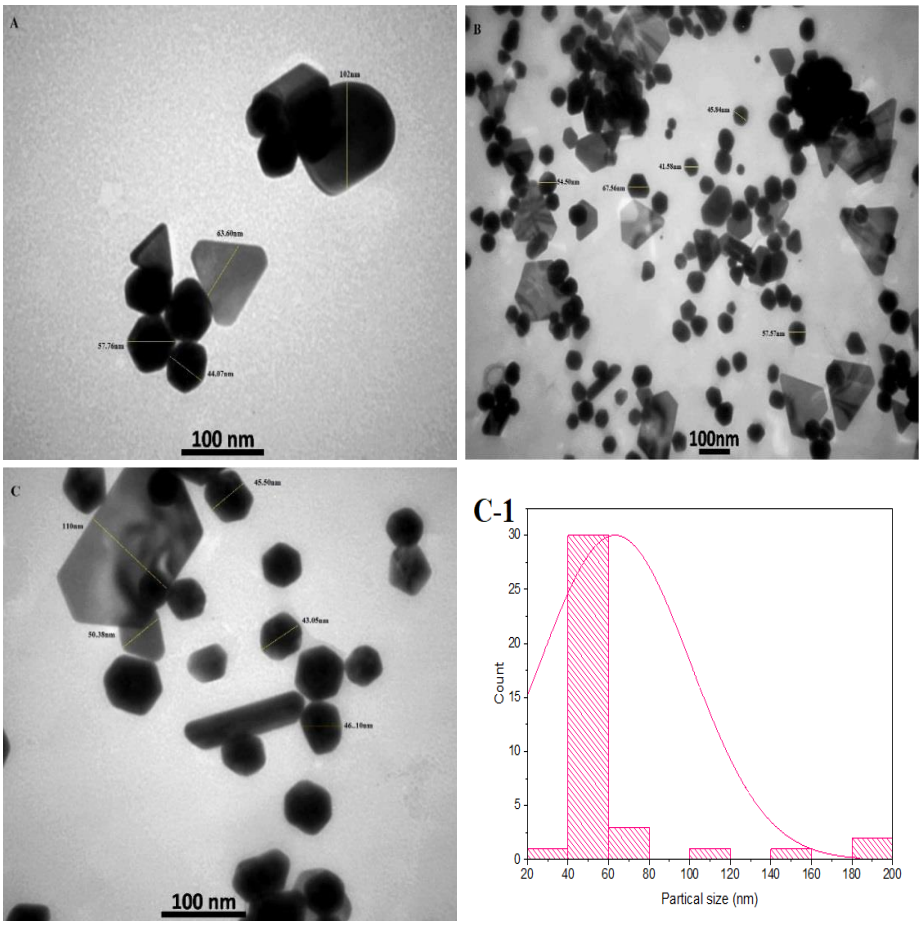

Figure 7: TEM analysis for (a, b, c) AuNPs-bromelain with 100nm scale bar (c-1) particle size distribution histogram.

3.2.4. Zeta Potential (ZP) Measurements

ZP is a quantitative measure of the net charge carried by particles in a medium; it indicates particle stability, with higher zeta potential values corresponding to greater stability. The zeta potential of nanoparticles is typically associated with their colloidal stability [50].

ZP of gold nanoparticle bioconjugates (AuNP-bios) provide important information on the surface charge that is critical for many applications, including drug delivery, biosensing, and cell imaging. The ZP measurements (ZPMs) were conducted under an alternative electrical field at a high frequency. The Au-NPs had a zeta potential of +0.1±0.4 mV, while the AuNPs-Bromelain had a zeta potential of +1.2±3.0 mV, which is well within the range to avoid agglomeration, demonstrating the lack of nanoparticle aggregation following the conjugation, because there are more carboxylic groups involved in the conjugation. The results of this study are consistent with those of Polte et al. [49].

3.2.5. XRD Analysis

XRD is used to determine the purity of the phase and the crystalline structure. The crystalline phases of AuNPs, AuNPs-bromelain were investigated using XRD patterns, as shown in Fig. 9a, b. The analysis of the synthesized gold nanoparticles under study using XRD spectroscopy revealed that the obtained values are consistent with the Bragg reflections at an angle of 20° using JCPDS data file No. (04-0784) as a

standard reference, which suggests that the synthesized gold nanoparticles are crystalline in nature, of a face-centered cubic structure. After the Au^{+3} was completely reduced to Au, the AuNPs (Fig. 9 a) were produced by chemical reduction according to the XRD pattern. The acquired strong diffraction peaks at 2θ of 31.84°, 38.31°, 44.98°, and 77.55°, corresponding to 111, 200, 202, and 311, respectively, are the same as those reported for the standard gold metal (Au) (JCPDS, USA). The results obtained correlate with a wide range of earlier researches [50-55].

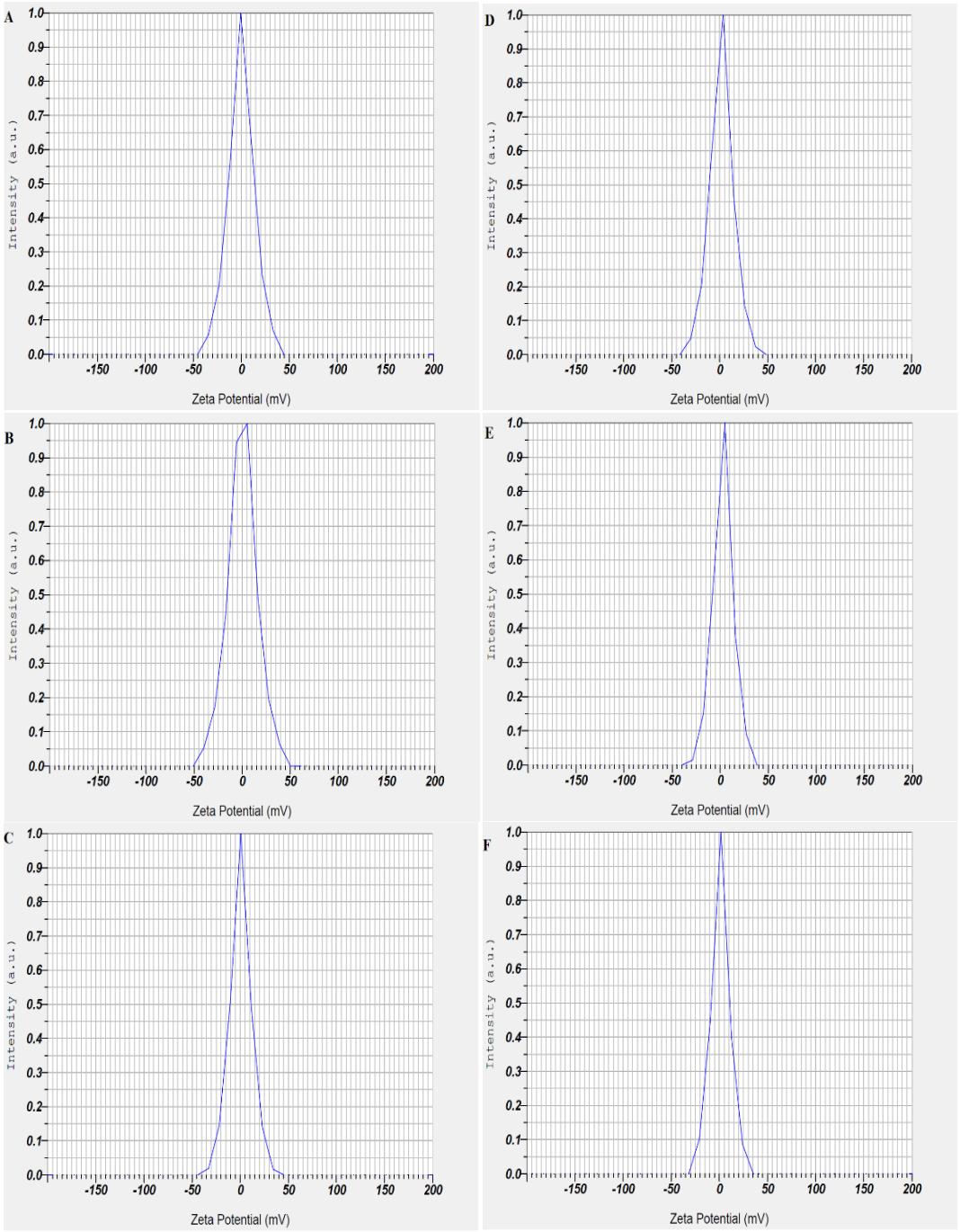

Figure 8: Zeta potential analysis (a, b, c) AuNPs, (d, e, f) AuNPs-bromelain.

According to Fig. 9b, the difference in the XRD peaks of AuNPs and AuNPs-Bromelain suggests that bromelain and AuNPs have coupled to create the AuNPs-Bromelain. According to the study's findings, bromelain loading on silver nanoparticles had no impact on their crystal structure. Abdul Latif et al. claimed that the additional

peaks in the XRD pattern were caused by biomolecules, such as phytochemical components, that were present on the surface of the nanoparticles. In some samples, these peaks were also caused by stabilizing agents like enzymes and proteins [56].

The AuNPs XRD pattern differed from that of the gold nanoparticle after loading bromelain. The appearance of additional peaks in the AuNPs-bromelain XRD pattern may indicated the association between bromelain and the gold nanoparticles. These additional peaks may be due to the presence of sodium tricitrate, which represents the reducing agent responsible for gold nanoparticle formation [57].

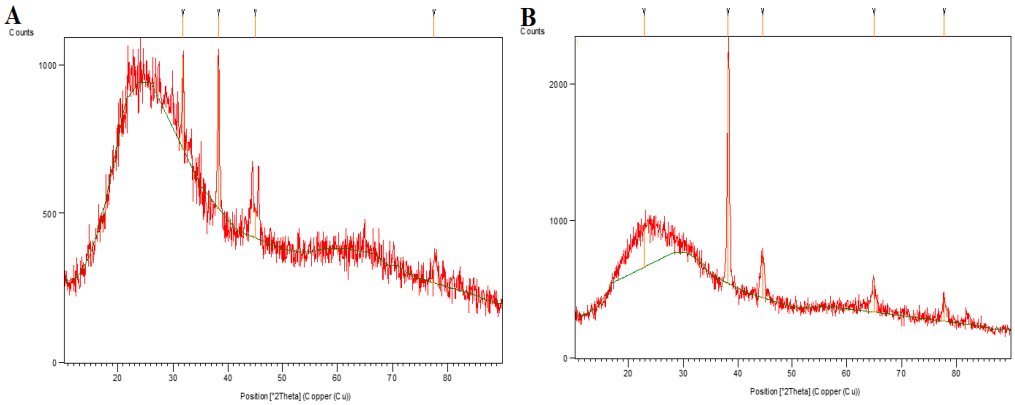

Figure 9: The XRD patterns, (a) AuNPs (b) AuNPs-bromelain.

4. Conclusions

Based on the obtained results, the following conclusions are reached: It is possible to incorporate photoprotein-analytical enzymes, such as bromelain, onto gold nanoparticles. Various characterization techniques were employed to ensure that the gold minutes associated with bromine are formed at the nanometer. This work presents a novel method for synthesizing AuNPs using bromelain as a reducing and capping agent.

Conflict of interest

Authors declare that they have no conflict of interest.

References

1. S. Bayda, M. Adeel, T. Tuccinardi, M. Cordani, and F. Rizzolio, Molecules **25**, 112 (2019). DOI: 10.3390/molecules25010112.
2. M. Saravanan, S. Arokiyaraj, T. Lakshmi, and A. Pugazhendhi, Microbi. Pathogen. **117**, 68 (2018). DOI: 10.1016/j.micpath.2018.02.008.
3. A. Pugazhendhi, D. Prabakar, J. M. Jacob, I. Karuppusamy, and R. G. Saratale, Microbi. Pathogen. **114**, 41 (2018). DOI: 10.1016/j.micpath.2017.11.013.
4. H. H. Al-Salhie and E. J. J. Al-Kalifawi, Biochem. Cell. Arch. **20**, 3991 (2020).
5. A. Pugazhendhi, T. N. J. I. Edison, I. Karuppusamy, and B. Kathirvel, Int. J. Pharmace. **539**, 104 (2018). DOI: 10.1016/j.ijpharm.2018.01.034.
6. M. A. Da Costa and F. J. Rios, Ore Geo. Rev. **148**, 105005 (2022). DOI: 10.1016/j.oregeorev.2022.105005.
7. J. Lou-Franco, B. Das, C. Elliott, and C. Cao, Nano-Micro Lett. **13**, 1 (2021). DOI: 10.1007/s40820-020-00532-z.
8. C. B. Poulie, E. Sporer, L. Hvass, J. T. Jørgensen, P. J. Kempen, S. I. Lopes Van Den Broek, V. Shalgunov, A. Kjaer, A. I. Jensen, and M. M. Herth, Chem. A European J. **28**, e202201847 (2022). DOI: 10.1002/chem.202201847.
9. K. Xia, T. Yatabe, K. Yonesato, S. Kikkawa, S. Yamazoe, A. Nakata, R. Ishikawa, N. Shibata, Y. Ikuhara, and K. Yamaguchi, Nat. Communic. **15**, 851 (2024). DOI: 10.1038/s41467-024-45066-9.
10. B. Merchant, Biologicals **26**, 49 (1998). DOI: 10.1006/biol.1997.0123.

11. S. Si, R. R. Bhattacharjee, A. Banerjee, and T. K. Mandal, Chem-A Euro. J. **12**, 1256 (2006). DOI: 10.1002/chem.200500834.
12. J.-J. Yuan, A. Schmid, S. P. Armes, and A. L. Lewis, Langmuir **22**, 11022 (2006). DOI: 10.1021/la0616350.
13. J. Kimling, M. Maier, B. Okenve, V. Kotaidis, H. Ballot, and A. Plech, J. Phys. Chem. B **110**, 15700 (2006). DOI: 10.1021/jp061667w.
14. N. E. Larm, J. B. Essner, K. Pokpas, J. A. Canon, N. Jahed, E. I. Iwuoha, and G. A. Baker, J. Phys. Chem.y C **122**, 5105 (2018). DOI: 10.1021/acs.jpcc.7b10536.
15. T. Ahmad, J. Nanotech. **2014**, 954206 (2014). DOI: 10.1155/2014/954206.
16. S. Hassan, F. Adam, M. R. Abu Bakar, and S. K. Abdul Mudalip, J. Saudi Chem. Soci. **23**, 239 (2019). DOI: 10.1016/j.jscs.2018.07.002.
17. M. Brust, M. Walker, D. Bethell, D. J. Schiffrin, and R. Whyman, Journal of the Chemical Society, Chemical Communications, 801 (1994). DOI: 10.1039/C39940000801.
18. S. I. Hussein, S. S. Shubber, and N. Y. Yaseen, Iraqi J. Veter. Medic. **43**, 17 (2019). DOI: 10.30539/iraqijvm.v43i2.525.
19. H. F. Al-Azzawie and L. A. Yaaqoob, Int. J. Res. Biotech. Biochem. **6**, 12 (2016).
20. M. M. Al-Musawi, G. A. Al-Bairuty, and H. S. Al-Shmgani, Ann. of Bio. **38**, 317 (2022).
21. R. M. Heinicke and W. A. Gortner, Econom. Bot. **11**, 225 (1957). DOI: 10.1007/BF02860437.
22. M. Livio, M. Bertoni, and G. J. Degaetano, Drugs Exp. Clin. Res. **4**, 49 (1978).
23. P. Shiew, Y. Fang, and F. Majid, Proceedings of the 3rd International Conference on Biotechnology for the Wellness Industry (Kuala Lumpur, Malaysia 2010). p. 8.
24. S.-Y. Wu, W. Hu, B. Zhang, S. Liu, J.-M. Wang, and A.-M. Wang, J. Surgic. Res. **176**, 503 (2012). DOI: 10.1016/j.jss.2011.11.1027.
25. J. Dong, P. L. Carpinone, G. Pyrgiotakis, P. Demokritou, and B. M. Moudgil, KONA Pow. Part. J. **37**, 224 (2020). DOI: 10.14356/kona.2020011.
26. H. S. Al-Shmgani, W. H. Mohammed, G. M. Sulaiman, and A. H. Saadoon, Artif. Cel. Nanomedic. Biotech. **45**, 1234 (2017). DOI: 10.1080/21691401.2016.1220950
27. P. Mulvaney, M. Giersig, and A. Henglein, J. Phys. Chem. **97**, 7061 (1993). DOI: 10.1021/j100129a022.
28. J. Jana, M. Ganguly, and T. Pal, RSC advances **6**, 86174 (2016). DOI: 10.1039/C6RA14173K.
29. N. N. Long, C. D. Kiem, S. C. Doanh, C. T. Nguyet, P. T. Hang, N. D. Thien, and L. M. Quynh, Journal of Physics: Conference Series (IOP Publishing, 2009). p. 012026.
30. S. R. Guntur, N. S. Kumar, M. M. Hegde, and V. R. Dirisala, Analyt. Chem. Insigh. **13**, 1 (2018). DOI: 10.1177/1177390118782877.
31. A. C. Pereira, A. E. Oliveira, M. A. Resende, and L. F. Ferreira, Analytica **4**, 250 (2023). DOI: 10.20944/preprints202305.1494.v1.
32. N. G. Bastús, J. Piella, and V. Puntes, Langmuir **32**, 290 (2016). DOI: 10.1021/acs.langmuir.5b03859.
33. W. Haiss, N. T. K. Thanh, J. Aveyard, and D. G. Fernig, Analyt. Chem. **79**, 4215 (2007). DOI: 10.1021/ac0702084.
34. H. Tyagi, A. Kushwaha, A. Kumar, and M. Aslam, Nanoscal. Res. Lett. **11**, 1 (2016). DOI: 10.1186/s11671-016-1576-5.
35. G. Sharma, A. R. Sharma, R. Bhavesh, J. Park, B. Ganbold, J.-S. Nam, and S.-S. Lee, Molecules **19**, 2761 (2014). DOI: 10.3390/molecules19032761.
36. R. K. Tekade, *Biomaterials and Bionanotechnology* (London, UK, Academic Press, 2019).
37. A. M. Mohammed and M. T. Sultan, Ibn AL-Haitham J. Pur. Appl. Sci. **33**, 55 (2020). DOI: 10.30526/33.3.2473.
38. A. M. Mohammed and M. T. Sultan, Ibn AL-Haitham Journal For Pure and Applied Sciences **33**, 55 (2020). DOI: 10.30526/33.3.2473.
39. A. Parodi, S. G. Haddix, N. Taghipour, S. Scaria, F. Taraballi, A. Cevenini, I. K. Yazdi, C. Corbo, R. Palomba, S. Z. Khaled, J. O. Martinez, B. S. Brown, L. Isenhart, and E. Tasciotti, ACS Nano **8**, 9874 (2014). DOI: 10.1021/nn502807n.
40. M. Sharma and R. Sharma, RSC Advances **8**, 2541 (2018). DOI: 10.1039/C7RA13555F.
41. A. J. Abdulghani and S. K. Mohuee, Iraqi J. Sci. **56**, 2425 (2015).
42. R. Bélteki, L. Kuklis, G. Gombár, D. Ungor, and E. Csapó, Chem. A European J. **29**, e202300720 (2023). DOI: 10.1002/chem.202300720.
43. M. S. Frost, M. J. Dempsey, and D. E. Whitehead, Coll. Surf. A Physicochem. Eng. Aspec. **518**, 15 (2017).
44. S. N. Hawar, H. S. Al-Shmgani, Z. A. Al-Kubaisi, G. M. Sulaiman, Y. H. Dewir, and J. J. Rikisahedew, J. Nanomat. **2022**, 1058119 (2022). DOI: 10.1155/2022/1058119.
45. P. Bhatnagar, A. B. Pant, Y. Shukla, B. Chaudhari, P. Kumar, and K. C. Gupta, European J. Pharmaceut. Biopharm. **91**, 35 (2015). DOI: 10.1016/j.ejpb.2015.01.015.

46. A. H. Al Dujaily and A. K. Mahmood, Iraqi J. Veter. Sci. **35**, 73 (2021). DOI: 10.33899/ijvs.2021.131415.1946.
47. A. Y. Jassim, J. Wang, K. W. Chung, F. Loosli, A. Chanda, G. I. Scott, and M. Baalousha, Coll. Surf. B Biointer. **209**, 112173 (2022). DOI: 10.1016/j.colsurfb.2021.112173.
48. M. Sharma and D. Chaudhary, Int. J. Pharmac. **594**, 120176 (2021). DOI: 10.1016/j.ijpharm.2020.120176.
49. J. Polte, X. Tuaev, M. Wuithschick, A. Fischer, A. F. Thuenemann, K. Rademann, R. Kraehnert, and F. Emmerling, ACS Nano **6**, 5791 (2012).
50. B. Marie, Ph.D Thesis, College of London, 2017.
51. Y. Nur, Ph.D. Thesis, University of Birmingham, 2013.
52. M. T. A. Alnuaimi, H. S. Al-Hayanni, and Z. Z. Aljanabi, Malaysian J. Microbio. **19**, 74 (2023). DOI: 10.21161/mjm.220060
53. H. Q. Hameed, A. A. Hasan, and R. M. Abdullah, Indian J. Publ. Heal. Res. Develop. **10**, 1218 (2019). DOI: 10.5958/0976-5506.2019.01459.1.
54. H. S. Hakeem and N. K. Abbas, Baghdad Sci. J. **18**, 0640 (2021). DOI: 10.21123/bsj.2021.18.3.0640.
55. M. H. A. Latif and Y. F. Mahmood, Ibn AL-Haitham J. Pur. Appl. Sci. **31**, 180 (2018). DOI: 10.30526/31.1.1865.
56. Y. Zhang, R. Huang, X. Zhu, L. Wang, and C. Wu, Chinese Sci. Bull. **57**, 238 (2012). DOI: 10.1007/s11434-011-4747-x.
57. R. Debnath, D. D. Purkayastha, S. Hazra, N. N. Ghosh, C. R. Bhattacharjee, and J. Rout, Mat. Lett. **169**, 58 (2016). DOI: 10.1016/j.matlet.2016.01.072.

بناء وتوصيف جسيمات الذهب النانوية والمحملة بالبروميلين

حنين ابراهيم علي[1]، بيداء حسين مطلك[1]

[1]قسم علوم الحياة، كلية التربية للعلوم الصرفة (أبن الهيثم)، جامعة بغداد، بغداد، العراق.

الخلاصة

حظيت عملية إنتاج واستخدام العناصر النانوية المعدنية، مثل الذهب، باهتمام كبير في الآونة الأخيرة بسبب سماتها المميزة ونطاق استخداماتها الواسع. وقد استخدمت معظم هذه الدراسات نهج توركيفيتش. وقد استخدم هذا البحث تقنية توركيفيتش لإنتاج جسيمات نانوية من الذهب (AuNPs). وقد تم توصيف جسيمات النانو الذهبية وجسيمات النانو الذهبية المحملة بالبروميلين باستخدام مجموعة متنوعة من الأساليب، بما في ذلك التحليل الطيفي فوق البنفسجي المرئي (UV-Vis)، والتحليل الطيفي بالأشعة تحت الحمراء بتحويل فورييه (FTIR)، والمجهر الإلكتروني الماسح بالانبعاث الميداني (FE-SEM)، وحيود الأشعة السينية (XRD)، والمجهر الإلكتروني النافذ (TEM)، وقياسات الجهد زيتا (ZP). كان لأطياف الأشعة فوق البنفسجية المرئية للبروميلين وجسيمات النانو الذهبية وجسيمات النانو الذهبية-بروميلين ذروة عند أطوال موجية 276 و534 و550 نانومتر على التوالي. وكشفت دراسات المجهر الإلكتروني الماسح بالانبعاث الميداني والمجهر الإلكتروني النافذ عن وجود جسيمات كروية ذات سطح أملس. تراوحت أقطار جسيمات النانو الذهبية من 49.32 إلى 77.29 نانومتر؛ وتراوحت أقطار جسيمات النانو الذهبية بروميلين من 46.39 إلى 75.66 نانومتر، كما تم تحديدها من خلال تحليل المجهر الإلكتروني الماسح FE-SEM. وأشار تحليل المجهر الإلكتروني النافذ إلى أن أحجام الجسيمات تراوحت من 7.40 إلى 15 نانومتر لجسيمات النانو الذهبية و14.51 نانومتر لجسيمات النانو الذهبية بروميلين. وكشفت أنماط حيود الأشعة السينية عن العديد من قمم الحيود، مما يدل على البنية البلورية للجسيمات النانوية المصنعة. وتم استخدام مطيافية الأشعة تحت الحمراء فورييه لتحديد المجموعات الوظيفية في الجسيمات النانوية المصنعة. وكشفت قياسات الجهد زيتا (ZP) أن جسيمات النانو الذهبية لها قيمة جهد زيتا +0.1±0.4، وكانت قيمة الجهد زيتا لجسيمات النانو الذهبية بروميلين +1.2±3.0 مللي فولت.

الكلمات المفتاحية: بروملين، جسيمات الذهب النانونيه، حيود الاشعه السينيه، جهد زيتا، المجهر الالكتروني النافذ